Structure and Magnetic Properties of Antiferromagnetic Manganese(III) Tetrakis(4-methoxyphenyl)porphyrin Tetracyanoethenide, [MnTOMePP][TCNE]·2PhMe, and Manganese(III) Tetrakis(2-fluorophenyl)porphyrin Tetracyanoethenide, [MnTFPP][TCNE]·2PhMe

Erik J. Brandon,[1a] Atta M. Arif,[1a] Brian M. Burkhart,[1b] and Joel S. Miller*,[1a]

Department of Chemistry, University of Utah, Salt Lake City, Utah 84112-0850, and the Hauptman−Woodward Medical Research Institute, Buffalo, New York 14203

Received August 22, 1997

The tetracyanoethylene (TCNE) electron-transfer salts of *meso*-tetrakis(4-methoxyphenyl)- and *meso*-tetrakis(2-fluorophenyl)porphinatomanganese(II), [MnTOMePP][TCNE]·2PhMe, **1**, and [MnTFPP][TCNE]·2PhMe, **2**, respectively, have been structurally and magnetically characterized. **1** and **2** belong to the triclinic $P\bar{1}$ (No. 2) space group [**1**, $a = 9.896(2)$ Å, $b = 10.256(3)$ Å, $c = 14.447(2)$ Å, $\alpha = 82.64(2)°$, $\beta = 92.40(1)°$, $\gamma = 109.07(2)°$, $T = -80$ °C, $Z = 1$, and $R(F_o) = 0.0295$; **2**, $a = 10.185(5)$ Å, $b = 11.081(3)$ Å, $c = 12.378(3)$ Å, $\alpha = 107.55(2)°$, $\beta = 82.88(3)°$, $\gamma = 111.09(3)°$, $T = -80$ °C, $Z = 1$, and $R(F_o) = 0.0421$]. **1** and **2** are coordination polymers with the Mn(III) sites bridged by *trans*-μ-σ-[TCNE]$^{\bullet-}$. The [TCNE]$^{\bullet-}$ is orientationally disordered in **2**, with the minor form being rotated by 90° with respect to the major form and in the same plane as the major form in an approximate 5:1 ratio. The Mn−N and intrachain Mn···Mn distances are 2.289 and 2.313 Å and 10.256 and 10.185 Å, and the Mn−N−C and the dihedral angle between the mean MnN_4−porphyrin and the mean [TCNE]$^{\bullet-}$ planes are 165.53 and 78.1° and 148.6 and 55.4° for **1** and the occupancy-weighted average of **2**, respectively. For **1** above 250 K the susceptibility can be fit by the Curie−Weiss expression with $\theta = -65$ K, while between 75 and 190 K an effective θ of +21 K is observed; for **2** above 225 K, θ is −71 K, while between 40 and 100 K the effective θ is +45 K. The initial negative θ values along with minima in the $\chi T(T)$ data at 134 K (X = OMe) and 240 K (X = F) are consistent with antiferromagnetic coupling. One $\chi''(T)$ and two $\chi'(T)$ peaks are observed for both **1** and **2**. The higher temperature [∼10 K (**1**) and 12.5 K (**2**)] $\chi'(T)$ peaks are frequency independent, lack a corresponding $\chi''(T)$ absorption, and are assigned to a transition to an antiferromagnetic state. In contrast, the lower-temperature frequency dependent [5.6 K (**1**) and 7.5 K (**2**) at 10 Hz] $\chi'(T)$ peaks have a corresponding frequency dependent $\chi''(T)$ peaks and are assigned to the transition to a spin-glass or superparamagnetic state. The T_c's are defined as $\chi'(T)$ data taken at 10 Hz and are listed above.

Introduction

The study of molecule-based magnets is an area of increasing contemporary interdisciplinary research.[2,3] One class of molecule-based magnets is exemplified by [MnTPP]$^+$[TCNE]$^{\bullet-}$ (TPP = *meso*-tetraphenylporphinato), an extended linear chain (1-D) complex that was characterized to be a ferrimagnet with a 14 K T_c.[4] With the goal of identifying the importance of 1-D with respect to 3-D interactions, developing a structure−function relationship for this class of magnetic materials, as well as preparing new molecule-based magnets with enhanced T_c's, we have pursued the study of this class of compounds.

These initial observations prompted the preparation and characterization of the related complexes [MnPc][TCNE] (H_2-Pc = phthalocycanine),[5] [MnOEP][TCNE] and [MnOEP]-$[C_4(CN)_6]$ (H_2OEP = octaethylporphyrin),[6] [MnTP′P][TCNE] (H_2TP′P = *meso*-tetrakis(3,5-di-*tert*-butyl-4-hydroxyphenyl)-porphyrin),[7] and [MnTTP][TCNQ] (TCNQ = 7,7,8,8-tetracyano-*p*-quinodimethane),[8] revealing the importance of uniformity in the chain structure to achieving strong intrachain magnetic interactions. To further correlate magnetic behavior with structural parameters, in particular by increasing the interchain separations with respect to [MnTPP][TCNE], we have undertaken the synthesis of the substituted TPP derivatives, [Mn-

(1) University of Utah. (b) Hauptman−Woodward Medical Research Institute.

(2) (a) Proceedings of the conference *Ferromagnetic and High Spin Molecular Based Materials*; Miller, J. S., Dougherty, D. A., Eds. *Mol. Cryst. Liq. Cryst.* **1989**, *176*. (b) Proceedings of the conference *Molecular Magnetic Materials*; Kahn, O., Gatteschi, D., Miller, J. S., Palacio, F., Eds. *NATO ARW Mol. Magn. Mater.* **1991**, *E198*. (c) Proceedings of the conference *Chemistry and Physics of Molecular Based Magnetic Materials*; Iwamura, H., Miller, J. S., Eds. *Mol. Cryst. Liq. Cryst.* **1993**, *232/233*. (d) Proceedings of the conference *Molecule-Based Magnets*; Miller, J. S., Epstein, A. J., Eds. *Mol. Cryst. Liq. Cryst.* **1995**, *271−274*. (e) Proceedings of the conference *Molecular-Based Magnets*; Itoh, K., Miller, J. S., Takui, T., Eds. *Mol. Cryst. Liq. Cryst.* **1997**, *305−306*. (f) Turnbull, M. M., Sugimoto, T., Thompson, L. K., Eds. *ACS Symposium Series 644*; American Chemical Society: Washington, DC, 1996.

(3) Reviews. (a) Buchachenko, A. L. *Russ. Chem. Rev.* **1990**, *59*, 307; *Usp. Khim.* **1990**, *59*, 529. Kahn, O. *Struct. Bonding* **1987**, *68*, 89. Kahn, O. *Molecular Magnetism*; VCH Publishers: Weinheim, Germany, 1993. (b) Caneschi, A.; Gatteschi, D.; Sessoli, R.; Rey, P. *Acc. Chem. Res.* **1989**, *22*, 392. Gatteschi, D. *Adv. Mater.* **1994**, *6*, 635. (c) Miller, J. S.; Epstein, A. J.; Reiff, W. M. *Acc. Chem. Res.* **1988**, *21*, 114; *Science* **1988**, *240*, 40; *Chem. Rev.* **1988**, *88*, 201. Miller, J. S.; Epstein, A. J. *New Aspects of Organic Chemistry*; Yoshida, Z., Shiba, T., Ohsiro, Y., Eds.; VCH Publishers: New York, 1989; p 237. Miller, J. S.; Epstein, A. J. *Angew. Chem., Int. Ed. Engl.* **1994**, *33*, 385; *Angew. Chem.* **1994**, *106*, 399; *Adv. Chem. Ser.* **1995**, *245*, 161.

(4) Miller, J. S.; Calabrese, J. C.; McLean, R. S.; Epstein, A. J. *Adv. Mater.* **1992**, *4*, 498.

(5) Miller, J. S.; Vazquez, C.; Calabrese, J. C.; McLean, R. S.; Epstein, A. J. *Adv. Mater.* **1994**, *6*, 217.

(6) Miller, J. S.; Vazquez, C.; Jones, N. L.; McLean, R. S.; Epstein, A. J. *J. Mater. Chem.* **1995**, *5*, 707.

S0020-1669(97)01076-8 CCC: $15.00
Published on Web 05/13/1998

TOMePP][TCNE] (H_2TOMePP = *meso*-tetrakis(4-methoxyphenyl)porphyrin) and [MnTFPP][TCNE] (H_2TFPP = *meso*-tetrakis(2-fluorophenyl)porphyrin).

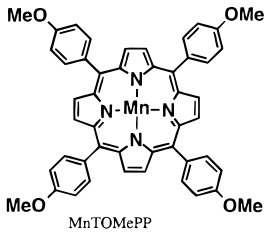

MnTOMePP

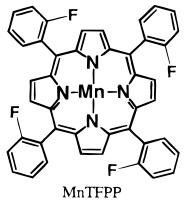

MnTFPP

Experimental Section

Synthesis. Solvents used in the preparation and purification of metalloporphyrins were used as received. Pyrrole was dried by vacuum distillation from CaH_2. TCNE was purified by vacuum sublimation. Substituted benzaldehydes (Aldrich) were used as received. Solvents used for the preparation of the [MnTXPP][TCNE] complexes were distilled under nitrogen from the appropriate drying agents before use.[9] Synthesis of these materials and all manipulations involving the TCNE radical anion were carried out in an inert atmosphere DriLab or using standard vacuum techniques. H_2TXPP (X = OMe, F) were prepared by a literature method.[10] [Mn^{III}TXPP][OAc] were prepared from H_2-TXPP and $Mn(OAc)_2·4H_2O$ and reduced to Mn^{II}TXPP(py) (py = pyridine) utilizing the methods described in the literature.[11] The $Mn(OAc)_2·4H_2O$ was dissolved in DMF and filtered prior to addition to the free-base porphyrin to avoid contamination with paramagnetic impurities.

[MnTOMePP][TCNE]·2PhMe. Mn^{II}TOMePP(py) (299.4 mg, 0.3454 mmol) was dissolved in 35 mL of hot toluene, and the dark-green solution was filtered through a medium-glass frit funnel and washed through with 5 mL of fresh, hot toluene to redissolve excess porphyrin. An excess of TCNE (44.6 mg, 0.348 mg) was dissolved in 15 mL of toluene at room temperature, and the clear yellow solution was similarly filtered. The porphyrin and TCNE solutions were then mixed and allowed to stand at room temperature in an inert atmosphere DriLab for 3 days. The resulting dark green microcrystals were collected by vacuum filtration and washed with fresh, dry toluene. As drying under reduced pressure resulted in complete loss of the toluene of solvation, the samples were stored at −40 °C directly after isolation from the reaction mixture (with no drying) to maintain the solvent content. Elemental analyses of this solvated material (which was not dried and was hermetically sealed in a tin capsule) were unsatisfactory; however, analysis of a dried sample was satisfactory. Anal. Calcd for $C_{54}H_{24}MnN_8O_4$ (no toluene): C, 70.82; H, 3.96; N, 12.23. Found: C, 70.86; H, 4.17; N, 11.99. IR (Nujol; cm^{-1}) υ_{CN}: 2205 m, 2163 s. Crystals suitable for X-ray diffraction were obtained by a modification of the above procedure in which a 1:1 dichloromethane/toluene solution (30 mL) of Mn^{II}TOMePP(py) (43.5 mg, 0.0502 mmol) was mixed with a 20 mL toluene solution of TCNE (10.0 mg, 0.0781 mmol). Upon standing for 2 days in a vibration-dampened glovebox, long, thin platelike crystals were harvested from the bottom of the crystallization flask. Separate single crystals dried for 1 and 0.5 h, respectively, were only weakly diffracting (even at low temperature) and unsuitable for a crystal structure determination. A desolvated sample isolated from a separate preparation that had been dried for 3 h displayed additional weak but well-defined IR stretches and resulted in a similar composition. IR (Nujol; cm^{-1}) υ_{CN}: 2203 m, 2186 w, 2161 s (2143 sh), 2121 w. Anal. Calcd for $C_{54}H_{24}MnN_8O_4$ (no toluene): C, 70.82; H, 3.96; N, 12.23. Found: C, 69.92; H, 4.13; N, 11.93.

[MnTFPP][TCNE]·2PhMe. Mn^{II}TFPP(py) (103.8 mg, 0.1268 mmol) was dissolved in 30 mL of toluene with magnetic stirring at room temperature, and the dark-red solution was filtered through a medium glass-frit funnel. TCNE (18.6 mg, 0.1452 mmol) was dissolved in 20 mL of toluene at room temperature, and the clear-yellow solution was similarly filtered. The two solutions were then mixed in an Schlenk flask, which was allowed to stand in an inert atmosphere glovebox for at least 3 days. The product (shiny, dark microcrystals) was collected by vacuum filtration, washed three times with 10 mL portions of fresh toluene, and dried under vacuum for 8 h (resulting in partial desolvation as reflected by elemental analysis). Anal. Calcd for $C_{58.75}H_{34}F_4MnN_8$ (for the 5/4 toluene solvate): C, 71.79; H, 3.49; N, 11.40. Found: C, 71.52; H, 3.77; N, 11.06. IR (Nujol; cm^{-1}) υ_{CN}: 2193 m, 2143 s cm^{-1}. Crystals suitable for X-ray diffraction were obtained by a modification of the above procedure in which a 20 mL toluene solution of TCNE (10.8 mg, 0.0843 mmol) was slowly layered by pipet transfer to a 1:1 dichloromethane/toluene solution (30 mL) of Mn^{II}TFPP(py) (43.7 mg, 0.0534 mmol). Upon standing for several days in a vibration-dampened glovebox, long, thin platelike crystals were harvested from the bottom of the crystallization flask.

Physical Methods. The 2−300 K magnetic susceptibility was determined on a Quantum Design MPMS-5XL 5 T SQUID (sensitivity = 10^{-8} emu or 10^{-12} emu/Oe at 1 T) magnetometer with an ultra-low-field (∼0.005 Oe) option, an ac option enabling the study of the ac magnetic susceptibility (χ' and χ'') in the range of 10−1000 kHz, reciprocating sample measurement system, and continuous low-temperature control with enhanced thermometry features. Samples were loaded in an airtight Delrin holder and packed with oven-dried quartz wool (to prevent movement of the sample in the holder). For isofield measurements, the samples were zero-field cooled (following oscillation of the dc field), and data were collected upon warming. For isothermal and ac measurements, remnant fluxes were minimized by oscillation of the dc field, followed by degaussing of the μ-metal shield and quenching of the magnet. Remaining fluxes were detected using a flux gate gaussmeter and further minimized by application of an opposing field, to bring the dc field to <0.5 Oe. In addition to subtraction of the sample holder, the core diamagnetic corrections of -695.7×10^{-6} and -632.3×10^{-6} emu/mol were used for the disolvates of **1** and **2**, respectively. Multiple samples were measured, to ensure reproducibility. The thermal properties were studied on a TA Instruments model 2050 thermogravimetric analyzer (TGA) (ambient to 550 °C) located in a Vacuum Atmospheres DriLab under nitrogen to study air- and moisture-sensitive samples. Samples were placed in aluminum pans and heated at 20 °C/min under a continuous 10 mL/min nitrogen flow. The infrared spectra (625−4000 cm^{-1}) were obtained on a Perkin-Elmer 783 spectrophotometer and on a Mattson Galaxy Series FTIR 3000 spectrophotometer. Elemental analyses were performed by Atlantic Microlabs (Norcross, GA). Deviations from calculated values may result from variations in solvent content and/or incomplete combustion of the porphyrin macrocycle.

X-ray Structural Analysis. X-ray data were collected at −80 °C on an Enraf-Nonius CAD4 diffractometer using Mo Kα radiation. Crystals of the [MnTXPP][TCNE] ditoluene solvates were covered with oil upon removal from the mother liquor, mounted on a glass fiber, and transferred to the goniometer where it was placed under a stream of nitrogen. The crystal structures were solved by direct methods and refined against F^2 using SHELXS. The key crystallographic information is listed in Table 1, and the atom coordinates for X = OMe and X = F are listed in Tables 2 and 3, respectively. Standard reflections showed no appreciable decay during data collection. Nonhydrogen atoms were refined anisotropically. Further refinement/analysis to locate disordered structural components was performed through examination of electron density difference maps as previously described.[12]

(7) Böhm, A.; Vazquez, C.; McLean, R. S.; Calabrese, J. C.; Kalm, S. E.; Manson, J. L.; Epstein, A. J.; Miller, J. S. *Inorg. Chem.* **1996**, *35*, 3083.
(8) (a) Dormann, E. *Synth. Met.* **1995**, *71*, 1781. (b) Winter, H.; Dormann, E.; Gompper, R.; Janner, R.; Kothrade, S.; Wagner, B.; Naarmann, H. *J. Magn. Magn. Mater.* **1995**, *140*−*144*, 1443. (c) Winter, H.; Klemen, M.; Dormann, E.; Gompper, R.; Janner, R.; Kothrade, S.; Wagner, B. *Mol. Cryst. Liq. Cryst.* **1995**, *273*, 111.
(9) Perrin, D. D.; Armarego, W. L. F. *Purification of Laboratory Chemicals*; Pergamon Press: Oxford, UK, 1988.
(10) Adler, A. D.; Longo, F. R.; Finarelli, J. D.; Goldmacher, J.; Assour, J.; Korsakoff, L. *J. Org. Chem.* **1967**, *32*, 476.
(11) Jones, R. D.; Summerville, D. A.; Basolo, F., *J. Am. Chem. Soc.* **1978**, *100*, 446.
(12) Burkhart, B. M.; Morin, B. G.; Epstein, A. J.; Calabrese, J. C.; Miller, J. S., Sundaralingham, M., submitted.

Table 1. Crystallographic Details for [Mn^{III}TXPP][TCNE]·2PhMe (X = OMe, F)

	X = OMe	X = F
empirical formula	$C_{68}H_{54}MnN_8O_4$	$C_{64}H_{40}F_4MnN_8$
a	9.896(2) Å	10.185 (5) Å
b	10.256(3) Å	11.081 (3) Å
c	14.447(2) Å	12.378 (3) Å
α	82.64(2)°	107.55 (2)°
β	92.40(1)°	82.88 (3)°
γ	109.07(2)°	111.09 (3)°
V	137.42 Å^3	1242.51 Å^3
Z	1	1
formula mass, daltons	1102.18	1052.02
space group	$P\bar{1}$ (No.2)	$P\bar{1}$ (No. 2)
T	−80 °C	−80 °C
λ	0.71073 Å	0.71073 Å
ρ_{calcd}	1.329 g cm^{-3}	1.406 g cm^{-3}
μ	2.861 cm^{-1}	3.188 cm^{-1}
$R(F_o)^a$	0.0295	0.0421
$R_w(F_o)^b$	0.0729	0.1062

^{a} $\sum(|F_o| - |F_c|)/\sum|F_o|$. ^{b} $\sum w(|F_o| - |F_c|)^2/\sum w|F_o|^2$.

The [TCNE]$^{\bullet-}$ disorder was detected through the use of difference electron density maps which illustrated a second orientation for [TCNE]$^{\bullet-}$ for **1**. The second orientation was fit with the aid of a graphics workstation, and the model was refined. The bonds and angles for the minor occupancy TCNE were restrained to match that of the major occupancy [TCNE]$^{\bullet-}$. The solvent disorder in **2** was detected through the use of difference electron density maps, which illustrated multiple solvent sites for the toluene. These orientations were fit with the aid of a graphics workstation and the model was refined. The bonds and angles for the solvent was restrained to a standard geometry throughout the refinement.

Results and Discussion

The reaction of Mn^{II}TOMePP(py) and Mn^{II}TFPP(py) with TCNE in toluene leads to dark-green [Mn^{III}TOMePP][TCNE]·2PhMe and [Mn^{III}TFPP][TCNE]·2PhMe, respectively. The infrared spectra of the ditoluene solvates in mineral oil mulls are consistent with the presence of [TCNE]$^{\bullet-}$, as indicated by the shifts to lower energy for υ_{CN} from 2259 s and 2221 m for neutral TCNE.[13] The key $\upsilon_{C\equiv N}$ absorptions at 2203 m and 2161 s cm^{-1} (**1**) and 2193 m and 2143 s cm^{-1} (**2**) confirm the presence of [TCNE]$^{\bullet-}$ and are inconsistent with [TCNE]^n [n = 0 (2259 s, 2221 m cm^{-1}), 2− (2104 s, 2069 s cm^{-1})].[13] These values are similar to the 2192 s and 2147 m cm^{-1} values reported for [MnTPP][TCNE][8] and 2197 s and 2133 m cm^{-1} for [MnTP′P][TCNE].[9] All [MnTXPP][TCNE]·2PhMe derivatives exhibit a higher-energy [TCNE]$^{\bullet-}$ nitrile absorption (2203−2191 cm^{-1}) which is virtually invariant, with the lower-energy absorption (2133−2163 cm^{-1}) spanning a larger range of energies (probably reflective of the bonded nitriles). The higher-energy υ_{CN} absorption is assigned the nonbonded nitrile groups, while the lower-energy absorption is assigned the Mn^{III}-bound nitriles.

Structure. The [Mn^{III}TOMePP]$^+$ and [Mn^{III}TFPP]$^+$ cations are comparable to other metallo-*meso*-tetraphenylporphinato complexes with the core being essentially planar with Mn−N distances 2.0077(15) and 2.0151(16) Å for **1**, 2.000(2) and 2.016(3) for **2**, and average 2.010 Å. The TCNE bond distances are characteristic of [TCNE]$^{\bullet-}$. The $(NC)_2C-C(CN)_2$ distances of 1.415(4) Å (**1**) and 1.406(8) Å (**2**) are longer but comparable to the distance reported for isolated [TCNE]$^{\bullet-}$ in [FeCp*$_2$][TCNE] (*i.e.*, 1.392 Å)[14] and 1.417 Å for [TCNE]$^{\bullet-}$ *trans*-*μ*-*N*-*σ*-bound to Mn^{III} in [MnTPP]$^+$[TCNE]$^{\bullet-}$,[4] but are distinctly longer than that reported for TCNE^0 (1.344 Å) and shorter than the 1.49 and 1.478 Å distances reported for [TCNE]$^{2-}$ in {[CoCp*$_2$]$^+$}$_2$[TCNE]$^{2-}$ [13] and [TCNE]$^{2-}$ *trans*-*μ*-*N*-*σ*-bound to Ir in [(Ph$_3$P)$_2$(OC)Ir]$_2$[TCNE], respectively.[13] [TCNE]$^{\bullet-}$ is essentially planar with a ∼2.0° (**1**) and 0.25° (**2**) twist; this is comparable to the 1.9° twist for [MnTPP]$^+$[TCNE]$^{\bullet-}$.[8]

Although evidence for structural disorder is not evident for **1** (except the solvent), cation and anion disorder, not solvent disorder, are observed for **2**. For **2**, two distinct occupancies of [TCNE]$^{\bullet-}$ were located with the minor form being rotated by 90° with respect to the major form and in the same plane as the major form, Figure 1b inset. The major form [79.5(11)%] and minor form [20.5(11)%] possess Mn−N$_{TCNE}$ separations of 2.309(12) and 2.33(4) Å and Mn−N−C angles of 150.3(14) and 140(5)°, respectively. The occupancy-weighted average Mn−N$_{TCNE}$ distance and Mn−N−C angle are 2.313 Å and 148.6°, respectively.

Due to the presence of an *o*-F group, the porphyrin phenyl rings exhibit disorder as well. The *o*-F-phenyl groups which partially sandwiches [TCNE]$^{\bullet-}$ is disordered over two sites in a 41%:59% ratio. These phenyl groups are also adjacent to one another through a different inversion with two identical F22 atoms within 3.09 Å of each other. This close contact is likely the source of this particular disorder to relieve steric interactions. The other *o*-F-phenyl's fluorine interacts with toluene on one side and is as close as 2.56 Å with a fluorine occupancy of 27%. Most likely, as the lattice is desolvated the toluene shifts to accommodate fluorine in this position. In the other position, this fluorine has an occupancy of 73% and points directly at [TCNE]$^{\bullet-}$ with a closest approach of 3.30 Å to the center carbon of both [TCNE]$^{\bullet-}$ orientations. Interestingly, the relative occupancies of the two forms of [TCNE]$^{\bullet-}$ are 80%:20% closely matching the 73%:27% disorder in the fluorines. Perhaps, the fluorine position is related to the [TCNE]$^{\bullet-}$ disorder.

The solid-state motif comprises parallel 1-D ···D$^+$A$^{\bullet-}$D$^+$A$^{\bullet-}$··· chains [D = MnTXPP (X = OMe, F); A = TCNE], Figure 2, where the [TCNE]$^{\bullet-}$ is *trans*-*μ*-*N*-*σ*-bound to Mn at a distance of 2.289(2) (**1**) and 2.309(12) Å (major form of **2**), and the Mn−N−C angle is 165.53(16) (**1**) and 150.3(14)° (major form of **2**). Static disorder associated with a rotated form of the anion as also exists in the [MnTPP][TCNE] material is not observed for **1** as no significant electron density was found proximate to the anion.

The Mn−N$_{TCNE}$ separations are comparable to that observed for [MnTPP][TCNE]·2PhMe [2.305 Å].[4] The Mn−N−C angles of 165.30° (**1**) and 148.6° (**2**) are 18.3° and 1.6° greater than the 147.0° angle reported for [MnTPP][TCNE]·2PhMe.[8] As a consequence, the intrachain Mn···Mn separation of 10.256 Å (**1**) and 10.185 Å (**2**) are 0.14 and 0.069 Å longer than the 10.116 Å distance observed for [MnTPP][TCNE]·2PhMe.[4] The TCNE−MnN$_4$ mean-plane dihedral angles are 78.1° (**1**), 55.6(3)° for the major orientation of **2**, and 53.9(16)° for the minor orientation of **2**. Thus, the orientation-weighted average dihedral angle for **2** is 55.4°, identical to that observed for [MnTPP][TCNE]·2PhMe.[8] In contrast, the dihedral angle for **1** is 22.7° greater than that observed for [MnTPP][TCNE]·2PhMe[8] and reduces the overlap between Mn d and [TCNE]$^{\bullet-}$ π^* orbitals.

In contrast to [MnTPP][TCNE], **1** possesses an interchain Mn···Mn separation of 9.869 Å, 0.36 Å shorter than the intrachain Mn···Mn separation. The other interchain Mn···Mn separations of 11.696, 14.447, and 16.611 Å are larger than the comparable 11.006, 11.823, and 13.269 Å distances for [MnTPP][TCNE].[4] As these distances strongly influence the

(13) Dixon D. A.; Miller, J. S. *J. Am. Chem. Soc.* **1987**, *109*, 3656.
(14) Miller, J. S.; Calabrese, J. C.; Dixon, D. A.; Epstein, A. J.; Bigelow, R. W.; Zhang, J. H.; Reiff, W. M. *J. Am. Chem. Soc.* **1987**, *109*, 769.

Table 2. Fractional Coordinates, $\times 10^4$, Isotropic Thermal Parameters, $\times 10^4$, and Site Occpancy for [MnTOMePP][TCNE]·2PhMe

atom	*x*	*y*	*z*	U_{iso}	occupancy	atom	*x*	*y*	*z*	U_{iso}	occupancy
Mn	0	0	0	211(1)	1	C43	−5790(20)	44934(19)	−01884(14)	279(4)	1
N1	18928(15)	11587(15)	−5871(10)	234(3)	1	C44	−17140(20)	48470(20)	−06484(15)	325(5)	1
N2	−8637(16)	−2488(15)	−12744(11)	240(4)	1	N45	−26250(20)	51570(20)	−10293(15)	495(5)	1
C1	31663(19)	17015(19)	−1263(13)	255(4)	1	C91	74470(30)	25680(30)	65010(20)	506(9)	0.878(5)
C2	33650(20)	16104(19)	8354(13)	258(4)	1	C92	86400(40)	31920(50)	59460(40)	629(13)	0.878(5)
C3	−22680(19)	−9557(19)	−14800(13)	258(4)	1	H92	95270	36330	62310	750	0.878(5)
C4	−24510(20)	−8910(20)	−24697(14)	334(5)	1	C93	85870(40)	31960(40)	50010(30)	722(12)	0.878(5)
H4	−33090	−13120	−27920	400	1	H93	94340	36240	46420	870	0.878(5)
C5	−11850(20)	−1250(20)	−28608(14)	346(5)	1	C94	73230(50)	25880(50)	45650(20)	664(11)	0.878(5)
H5	−9900	1020	−35110	420	1	H94	72790	26090	39060	800	0.878(5)
C6	−01850(20)	2881(19)	−21240(13)	265(4)	1	C95	61250(40)	19480(40)	51000(30)	704(11)	0.878(5)
C7	12360(20)	11250(20)	−22576(14)	275(4)	1	H95	52420	15080	48100	850	0.878(5)
C8	21960(20)	15064(19)	−15263(13)	258(4)	1	C96	61870(60)	19370(50)	60590(50)	650(40)	0.878(5)
C9	36820(20)	22780(20)	−16473(14)	310(5)	1	H96	53450	14860	64190	780	0.878(5)
H9	41650	26430	−22260	370	1	C97	75330(70)	25950(60)	75380(30)	745(14)	0.878(5)
C10	42720(20)	23940(20)	−07948(14)	315(5)	1	H97A	85380	29500	77260	1120	0.878(5)
H10	52480	28520	−6610	380	1	H97B	70960	16510	78520	1120	0.878(5)
C21	48514(19)	22310(20)	12004(13)	264(4)	1	H97C	70230	32000	77120	1120	0.878(5)
C22	56700(20)	13920(20)	14873(16)	363(5)	1	C91′	76700(300)	27600(300)	55290(130)	740(180)	0.056(6)
H22	52820	4220	14500	440	1	C92′	63500(300)	19300(400)	58800(150)	600(400)	0.056(6)
C23	70460(20)	19310(20)	18295(16)	368(5)	1	H92′	56190	15110	54580	710	0.056(6)
H23	75910	13350	20260	440	1	C93′	60500(200)	17000(400)	68110(160)	480(140)	0.056(6)
C24	76170(20)	33370(20)	18826(14)	308(5)	1	H93′	51310	11200	70270	570	0.056(6)
O24	89621(14)	39901(16)	22111(11)	418(4)	1	C94′	70700(300)	22900(400)	74380(150)	180(110)	0.056(6)
CM24	98390(20)	31520(30)	24980(17)	474(6)	1	H94′	68750	21220	80880	220	0.056(6)
HM2A	107880	37460	26700	710	1	C95′	83900(200)	31400(300)	71090(130)	70(80)	0.056(6)
HM2B	99290	26480	19840	710	1	H95′	90910	35940	75320	90	0.056(6)
HM2C	94020	24860	30380	710	1	C96′	86900(300)	33300(600)	61670(160)	500(300)	0.056(6)
C25	68210(20)	41920(20)	15903(15)	362(5)	1	H96′	96290	38670	59550	580	0.056(6)
H25	72150	51630	16210	430	1	C97′	79300(300)	30500(300)	44980(140)	1000(400)	0.056(6)
C26	54520(20)	36430(20)	12526(15)	331(5)	1	H97D	89580	33170	43780	1480	0.056(6)
H26	49140	42440	10530	400	1	H97E	75760	38060	42350	1480	0.056(6)
C31	17680(20)	16390(20)	−32352(14)	289(4)	1	H97F	74270	22110	42060	1480	0.056(6)
C32	18770(20)	7240(20)	−38420(15)	373(5)	1	C91″	70100(300)	24200(300)	53690(140)	590(150)	0.061(7)
H32	16150	−2400	−36270	450	1	C92″	62000(300)	18800(300)	61700(140)	500(400)	0.061(7)
C33	23540(20)	11850(20)	−47434(15)	406(5)	1	H92″	52410	12950	61150	600	0.061(7)
H33	24170	5400	−51430	490	1	C93″	67400(300)	21400(300)	70350(140)	540(140)	0.061(7)
C34	27430(20)	25890(20)	−50701(14)	359(5)	1	H93″	61570	17360	75700	650	0.061(7)
O34	32072(19)	29337(17)	−59727(10)	513(4)	1	C94″	81200(400)	29900(700)	71410(160)	1800(900)	0.061(7)
CM34	36540(30)	43500(30)	−63479(16)	526(6)	1	H94″	84840	32000	77410	2150	0.061(7)
HM3A	28700	47260	−63050	790	1	C95″	89500(300)	35200(500)	63620(160)	600(200)	0.061(7)
HM3B	39230	44360	−70040	790	1	H95″	99190	40850	64240	750	0.061(7)
HM3C	44790	48700	−59960	790	1	C96″	84000(300)	32400(400)	54860(150)	390(15)	0.061(7)
C35	26480(20)	35190(20)	−44857(14)	350(5)	1	H96″	90000	36200	49540	470	0.061(7)
H35	29120	44830	−47030	420	1	C97″	63800(400)	21100(500)	44290(160)	740(180)	0.061(7)
C36	21630(20)	30350(20)	−35755(14)	333(5)	1	H97G	71360	24650	39550	1110	0.061(7)
H36	21020	36810	−31760	400	1	H97H	56540	25690	42820	1110	0.061(7)
N41	−6000(18)	19790(18)	−00264(12)	341(4)	1	H97I	59390	11080	44330	1110	0.061(7)
C42	−6150(20)	31020(20)	−01131(14)	277(4)	1						

3-D ordering temperature, T_c is a strong function of the interchain interactions, and the larger distances suggest a reduced T_c. There is also a close contact interchain contact between the O(1)···C(11) of 3.167 Å and a 2.615 Å contact between O(1) and H(3) bound to C(10). The key intra- and interchain Mn···Mn separations for [MnTOMePP][TCNE]·2PhMe are presented in Table 4.

X-ray crystallography reveals the presence of up two toluene molecules per [MnTXPP][TCNE], *i.e.*, [MnTXPP][TCNE]·*y*PhMe ($y \leq 2$). These solvent molecules form "channels" between the chains, similar to other porphyrin intercalates.[15] Thermogravimetric analysis of this material indicates that slight variations in the degree of solvation occur from sample to sample (ca. 11−14 wt %, *i.e.*, $1.3 \leq y \leq 1.7$). However, for **1** the solvent is completely removed under reduced pressure at room temperature without altering the IR spectra, except for the loss of the absorption attributed to PhMe. For **2**, only partial desolvation occurs under the same conditions.

Magnetic Properties. The 2−300 K reciprocal corrected magnetic susceptibility, χ^{-1}, and moment, μ_{eff}, of [MnTXPP][TCNE]·2PhMe are presented in Figure 3. For X = OMe above 250 K the susceptibility of can be fit by the Curie−Weiss expression, $\chi \propto 1/(T - \theta)$, with $\theta = -65$ K, while between 75 and 190 K an effective θ of +21 K is observed. For X = F above 225 K $\theta = -71$ K, while between 40 and 100 K the effective θ is +45 K. The initial negative θ values along with minima in the $\chi T(T)$ data at 134 K (X = OMe) and 240 K (X = F) are consistent with ferrimagnetic linear chains as reported for [MnTP′P][TCNE] and [MnTPP][TCNE].[4,7] Due to the broadness of these minima as well as slight variations which occur between preparations (possibly due to anion disorder and/or variations in the precise solvent content), the accuracy of the minima positions is estimated at ±20 K. In contrast, neither negative θ values nor minima in the $\chi T(T)$ data (which presumably occur near or above 300 K) were observed for [MnTP′P][TCNE] or [MnTPP][TCNE] due to the stronger coupling of the chains relative to **1** and **2**. The observed room-temperature effective moments, μ_{eff} [$\equiv(8\chi T)^{1/2}$], of 4.88 μ_B (X = OMe) and 5.26 μ_B (X = F) are near the expectation of 5.20

(15) (a) Goldberg, I.; Krupitsky, H.; Stein, Z.; Hsiou, Y.; Strouse, C. E. *Supramol. Chem.* **1995**, *4*, 203. (b) Krupitsky, H.; Stein, Z.; Goldberg, I. *J. Inclusion Phenom. Mol. Recognition* **1995**, *20*, 211. (c) Goldberg, I. *Mol. Cryst. Liq. Cryst.* **1996**, *278*, 767. (d) Byrn, M. P.; Curtis, C. J.; Hsiou, Y.; Kahn, S. I.; Sawin, P. A.; Tendick, S. K.; Terzis, A.; Strouse, C. E. *J. Am. Chem. Soc.* **1993**, *115*, 9480. (e) Bryn, M. P.; Curtis, C. J.; Khan, S. O.; Sawain, P. A.; Tsurumi, R.; Strouse, C. E. *J. Am. Chem. Soc.* **1990**, *112*, 1865.

Table 3. Fractional Coordinates, $\times 10^4$, Isotropic Thermal Parameters, and Site Occpancy for [MnTFPP][TCNE]·2PhMe

atom	*x*	*y*	*z*	U_{iso}	occupancy	atom	*x*	*y*	*z*	U_{iso}	occupancy
Mn	5000	5000	5000	192(2)	1	C24	7884(4)	11570(3)	3166(3)	322(9)	1
N1	6159(3)	6927(3)	5735(2)	212(6)	1	H24	8244	12374	2936	390	1
N2	4859(3)	5516(2)	3614(2)	207(6)	1	C25	8794(4)	10986(3)	3338(3)	317(8)	1
C1	6767(3)	7416(3)	6787(3)	227(7)	1	H25	9779	11384	3234	380	1
C2	6676(3)	6685(3)	7534(3)	230(7)	1	C26	8252(4)	9808(3)	3665(3)	284(8)	1
C3	4110(3)	4680(3)	2647(3)	237(7)	1	H26	8881	9401	3781	340	0.413(6)
C4	4281(4)	5417(3)	1848(3)	305(8)	1	F26	9093(3)	9209(4)	3775(3)	411(13)	0.587(6)
H4	3887	5069	1114	370	1	N41	2875(10)	5308(18)	5599(17)	320(30)	0.795(11)
C5	5099(4)	6693(3)	2315(3)	305(8)	1	C42	1696(5)	5032(6)	5468(4)	256(12)	0.795(11)
H5	5388	7412	1974	370	1	C43	245(4)	4686(4)	5307(4)	292(14)	0.795(11)
C6	5453(3)	6767(3)	3423(3)	222(7)	1	C44	−704(13)	3694(12)	5813(13)	390(30)	0.795(11)
C7	6255(3)	7937(3)	4193(3)	226(7)	1	N45	−1458(8)	2898(6)	6216(5)	554(17)	0.795(11)
C8	6568(3)	7996(3)	5275(3)	209(7)	1	N41′	2940(30)	5490(70)	5600(50)	130(70)	0.205(11)
C9	7402(3)	9191(3)	6071(3)	253(8)	1	C42′	1909(7)	5390(20)	5237(18)	200(50)	0.205(11)
H9	7791	10069	5972	300	1	C43′	665(6)	5437(11)	4886(12)	210(50)	0.205(11)
C10	7526(3)	8824(3)	6987(3)	266(8)	1	C44′	810(30)	6440(40)	4330(50)	190(90)	0.205(11)
H10	8032	9403	7652	320	1	N45′	920(30)	7236(19)	3890(20)	450(70)	0.205(11)
C31	7528(4)	7360(3)	8587(3)	256(8)	1	C91	2281(4)	5835(4)	9139(3)	437(10)	1
C32	7138(4)	8172(4)	9539(3)	389(10)	1	C92	3044(4)	6932(4)	8734(3)	432(10)	1
H32	6279	8326	9537	470	0.728(7)	H92	3273	6796	7949	520	1
F32	6076(9)	8512(11)	9509(9)	760(40)	0.272(7)	C93	3474(5)	8212(5)	9455(4)	503(11)	1
C33	7936(5)	8781(4)	10509(3)	432(10)	1	H93	3981	8953	9161	600	1
H33	7626	9335	11159	520	1	C94	3180(5)	8429(5)	10591(4)	537(12)	1
C34	9171(4)	8574(4)	10514(3)	412(10)	1	H94	3484	9317	11086	640	1
H34	9732	8994	11172	490	1	C95	2436(5)	7349(6)	11015(4)	598(13)	1
C35	9618(4)	7765(4)	9579(3)	402(10)	1	H95	2238	7489	11805	720	1
H35	1481	7620	9586	480	1	C96	1980(5)	6057(5)	10280(4)	500(11)	1
C36	8783(4)	7163(3)	8625(3)	308(8)	1	H96	1453	5317	10572	600	1
H36	9085	6597	7978	370	0.272(7)	C97	1775(5)	4434(5)	8330(4)	604(13)	1
F36	9208(3)	6411(3)	7740(2)	429(11)	0.728(7)	H97A	2092	4477	7557	910	0.5
C21	6821(4)	9203(3)	3829(3)	239(7)	1	H97B	744	4069	8360	910	0.5
C22	5942(3)	9829(3)	3652(3)	280(8)	1	H97C	2161	3851	8549	910	0.5
H22	4956	9439	3761	340	0.587(6)	H97D	1239	3788	8753	910	0.5
F22	4605(4)	9252(5)	3747(5)	397(18)	0.413(6)	H97E	2587	4196	7951	910	0.5
C23	6454(4)	11001(4)	3323(3)	337(9)	1	H97F	1171	4413	7762	910	0.5
H23	5828	11410	3207	400	1						

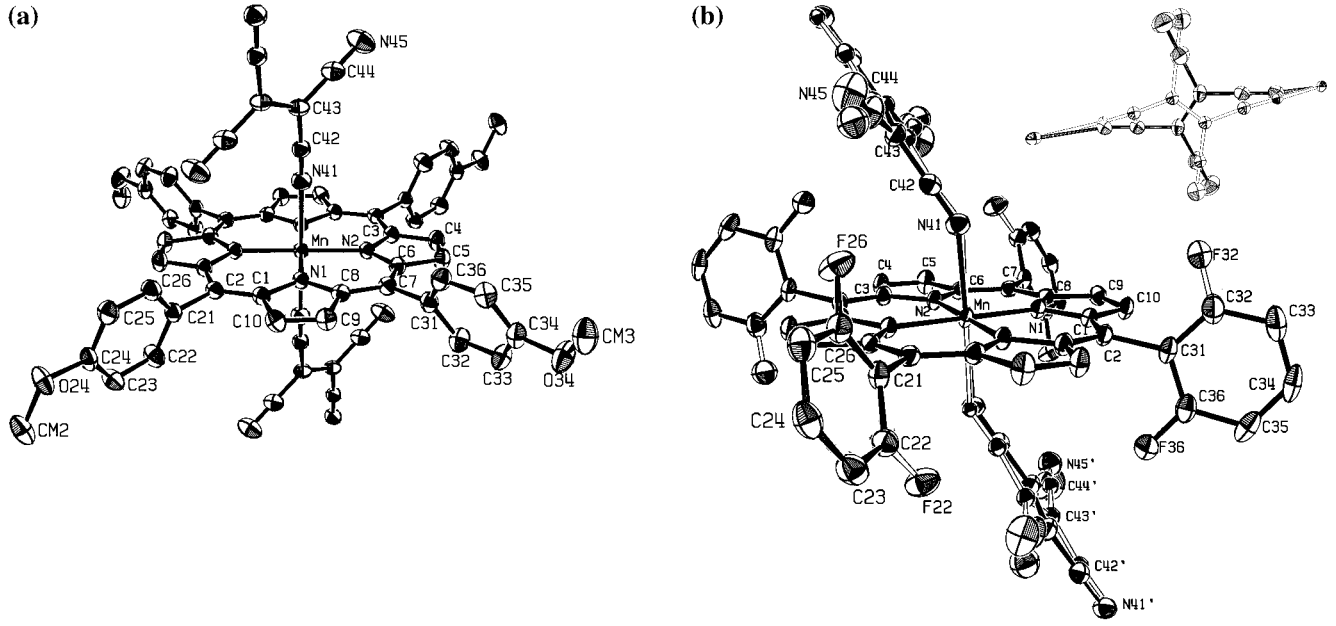

Figure 1. ORTEP (50%) atom labeling diagram for centrosymmetic $[Mn^{III}TOMePP]^+[TCNE]^{\bullet-}\cdot 2PhMe$ (a) and $[Mn^{III}TFPP]^+[TCNE]^{\bullet-}\cdot 2PhMe$ (b) showing the cation and the anion. The inset shows the disordered $[TCNE]^{\bullet-}$ for $[Mn^{III}TFPP]^+[TCNE]^{\bullet-}\cdot 2PhMe$.

μ_B for isotropic independent $g = 2$, $S = 2$, and $S = {}^1/_2$ radicals, as is observed for [MnTPP][TCNE] and [MnTP′P][TCNE]. Slight deviations may be attributable to variations in solvent content and/or interactions between the cation and anion at room temperature. At lower temperature the moment increases due to correlation of the uncompensated moment, reaching a maximum at 14 μ_B at 8 K (X = OMe) and 33 μ_B at 12 K (X = F) before dropping in value due to the onset of saturation and zero-field splitting. [MnTOMePP][TCNE]·2PhMe does not exhibit saturation at 5 K at fields as high as 5 T, and no hysteresis was observed at 5 K. [MnTFPP][TCNE]·2PhMe exhibits a saturation magnetization at 5 K of 17 786 emu Oe/mol (5 T) in accord with the expectation of antiferromagnetic coupling, *i.e.*, 16 755 emu G/mol for the $S_{Tot} = 2 - {}^1/_2$ system,

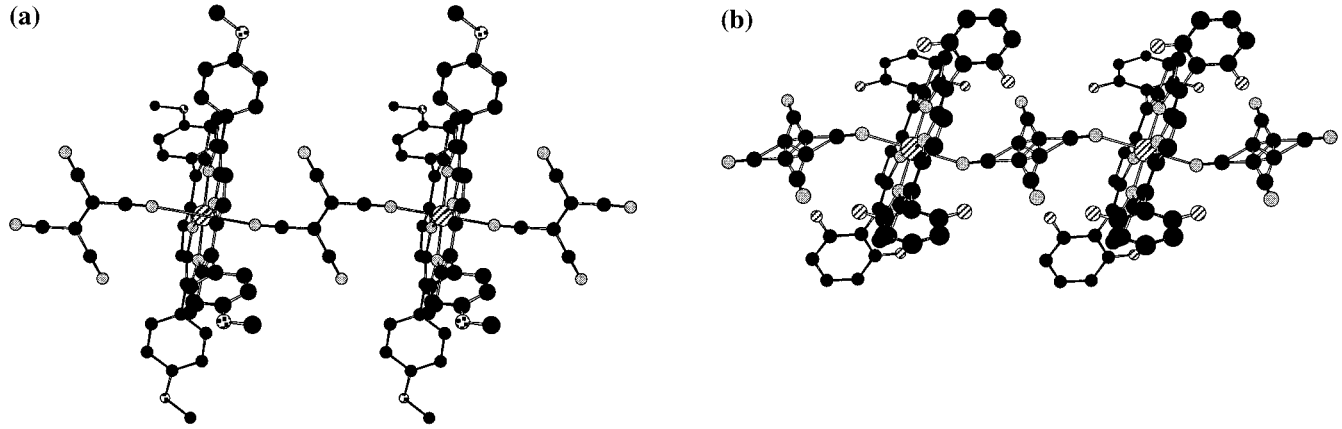

Figure 2. (a) View parallel the *b* (chain axis) for [Mn^{III}TOMePP][TCNE]·2PhMe, **1**. (b) View parallel to *a* (chain axis) for [Mn^{III}TFPP][TCNE]·2PhMe, **2**.

Table 4. Intra- and Interchain Mn···Mn and Chain Separations for [Mn^{III}TXPP][TCNE]·2PhMe (X = OMe, F, H)

	X = F	X = OMe	X = H[4]
intrachain Mn···Mn, Å	10.185	10.256	10.116
interchain Mn···Mn, Å			
in-registry	12.378, 13.903, 15.023, 15.718	14.447, 16.611, 17.166, 18.758	13.296, 14.932
out-of-registry	11.081, 12.054	9.896, 11.696, 17.850, 17.875	11.006, 11.823, 13.838, 15.667
interchain Mn···Mn/Mn···Mn, Å			
in-registry	12.286, 13.683	14.362, 17.115	13.139
out-of-registry	10.345	9.266, 17.111	10.210, 13.630

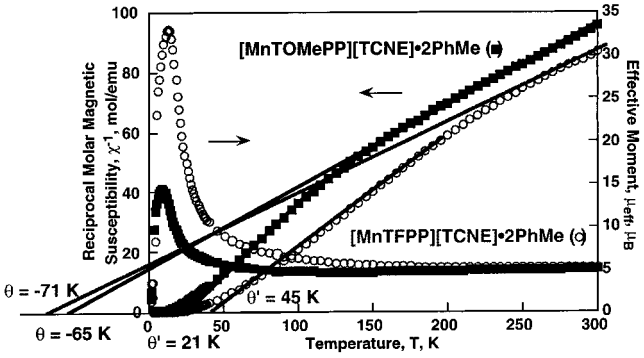

Figure 3. Reciprocal molar magnetic susceptibility, χ^{-1}, and moment, μ, as a function of temperature for (a) polycrystalline [Mn^{III}TOMePP]$^+$[TCNE]$^{\bullet-}$·*y*PhMe (○) and (b) polycrystalline [Mn^{III}TFPP]$^+$[TCNE]$^{\bullet-}$·*y*PhMe (■). The moment is $(8\chi T)^{1/2}$ where χ is taken as M(0.1 T)/0.1 T.

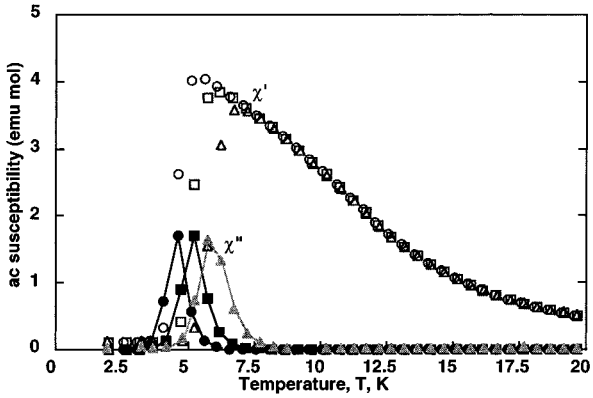

Figure 4. Real, χ' (○, □, △), and imaginary ac susceptibility, χ'' (●, ■, ▲), as a function of temperature taken at 10, 100, and 997 Hz at zero-applied dc field (<0.5 Oe) and a 1 Oe applied ac field for polycrystalline [Mn^{III}TOMePP]$^+$[TCNE]$^{\bullet-}$·2PhMe, **1**.

which is substantially lower than expected for ferromagnetic coupling, *i.e.*, 27 925 emu G/mol for the $S_{Tot} = 2 + {}^1/_2$ system. Hysteresis is not observed at 5 K but is present at 2 K. The coercive field is not reproducible and varies with samples history, which leads to differing degrees of domain wall pinning. Hence its value, which can be as high as 0.5 T, is not reported.

The presence of minima in the $\chi T(T)$ and moment data are indicative of ferrimagnetic chains composed of antiferromagnetically coupled $S = 2$ and $S = {}^1/_2$ spin sites. The minima occur at 134 and 240 K for **1** and **2**, respectively. An analytical function developed for exchange-coupled alternating quantum/classical spin sites (*i.e.*, the Seiden expression[16]) within independent chains did not provide satisfactory fits of the data for **1** or **2**. Nonetheless, using the approximation of $J = -T_{min}/4.2$,[17] J is −32 and −64 K for **1** and **2**, respectively. From the relative positions of the minima (separated by ∼110 K), the intrachain coupling is stronger for **2**.

To determine T_c the temperature dependence of the zero-field cooled ac susceptibility was examined, and reveals two peaks the in-phase (χ') and only one peak in the out-of-phase (χ'') components for **1** and **2**, Figures 4 and 5. For both **1** and **2** the higher-temperature $\chi'(T)$ peak is frequency independent and lacks a corresponding χ'' absorption. Hence, these ordering temperatures at ∼10 K for **1** and 12.5 K for **2** are characteristic of a transition to an antiferromagnetic state as observed for [MnOEP][C_4(CN)$_6$].[6] In contrast, the lower-temperature frequency-dependent $\chi'(T)$ peaks have a corresponding frequency-dependent $\chi''(T)$ peaks indicative of disorder/frustration in the spin-lattice and either spin-glass or superparamagnetic behavior.[18] Further detailed studies are needed to understand this transition. The T_c, defined as the peak in the $\chi'(T)$ data taken at 10 Hz, is 5.6 K (**1**) and 7.5 K (**2**) for this second transition. The probable source of the frustration, previously attributed to anion disorder in [MnTPP][TCNE],[12] is present in **2** but not in

(16) Seiden, J. *J. Phys. Lett.* **1983**, *44*, L947.
(17) Drillion, M.; Coronado, E.; Georges, R.; Gianduazzo, J. C.; Curely, J. *Phys. Rev. B* **1989**, *40*, 10 992.
(18) Mydosh, J. A. *Spin Glasses*; Francois and Taylor: Washington, DC, 1993.

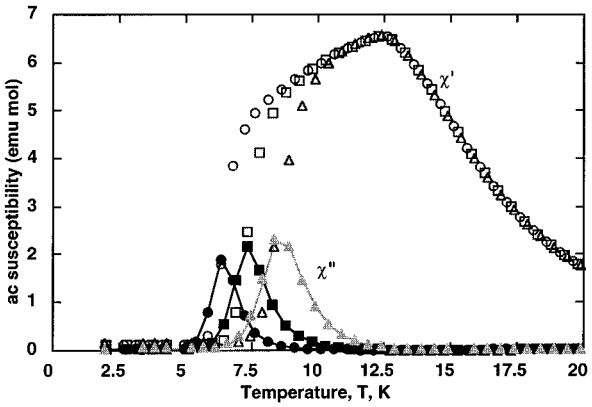

Figure 5. Real, χ' (○, □, △), and imaginary ac susceptibility, χ'' (●, ■, ▲), as a function of temperature taken at 10, 100, and 997 Hz at zero-applied dc field (<0.5 Oe) and a 1 Oe applied ac field for polycrystalline $[Mn^{III}TFPP]^{+}[TCNE]^{\bullet-}\cdot 2PhMe$, **2**.

1; however, **1** has a disordered solvent which may contribute to the spin-glass behavior. Disorder below ∼15% cannot be ascertained by crystallographic methods, and may be present.

Conclusion

Two substituted derivatives of the molecule-based magnet [MnTXPP][TCNE]·2PhMe have been prepared and structurally and magnetically characterized; ferrimagnetic behavior with a crossover to 3-D magnetic order has been observed in both cases. Comparison of the effective θ values for **1** and **2** with the previously characterized [MnTP′P][TCNE] or [MnTPP][TCNE] magnets indicate pronounced variations in the temperature-dependent magnetic behavior. The position of the minima in the $\chi T(T)$ data, which varies for all four of these compounds from ca. 134 K to above 300 K, suggests the intrachain coupling strength between Mn^{III} and $[TCNE]^{\bullet-}$ may therefore be controllable through modification of the ancillary porphyrin ligand. We are currently developing a structure−function relationship for this class of materials based on semiempirical calculations of metal−radical overlap.

Acknowledgment. The authors appreciate the constructive comments and insight provided by Prof. E. Coronado (Universidad de Valencia), Prof. A. J. Epstein, Dr. C. M. Wynn, and Mr. M. Girtu (The Ohio State University) and gratefully acknowledge the support from the National Science Foundation (Grant No. CHE9320478).

Supporting Information Available: A summary of the crystallographic data, tables of fractional coordinates and isotropic thermal parameters, anisotropic thermal parameters, bond distances and angles for [MnTOMePP][TCNE]·2PhMe and [MnTFPP][TCNE]·2PhMe (18 pages). Ordering information is given on any current masthead page.

IC9710768